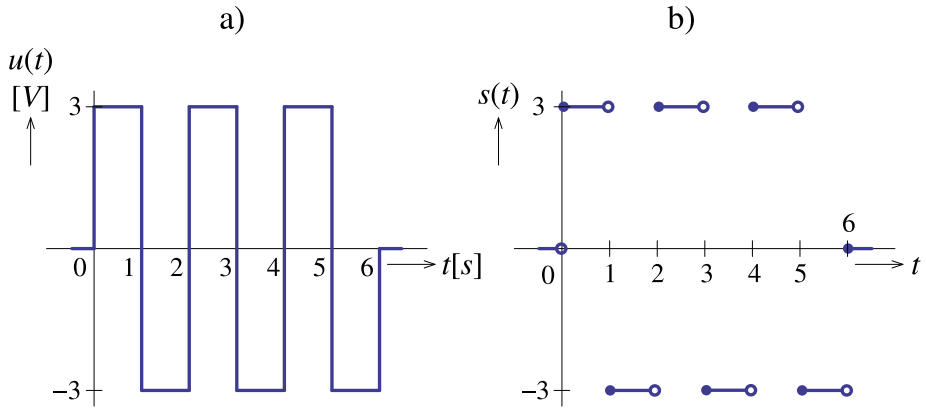

Figure 1.1: a) Real signal displayed on the oscilloscope screen, b) mathematical model of the real signal

There is a kind of convention that the instantaneous signal values (voltage $u(t)$, current $i(t)$, etc.) are denoted in lower-case italic type while the constant signal values are written in capital type (constant K, magnitude U, etc.). The conjunction symbol $\wedge$ means that the signal values hold for times given by all conditions.

1.2 Classification of signals

Signals (their mathematical models) can be classified according to their certain properties. The basic classification of signals according to the randomness of their waveform is into

– deterministic signals
– random signals

Deterministic signals (determined, regular) are signals that have a known value of the dependent variable for every value of the independent variable. Their waveform is defined by a known function or sequence, e.g. $\cos x$, $\ln x$, etc. Deterministic signals are further classified into

– periodic deterministic signals
– non-periodic deterministic signals

A signal (function) $s(t)$ is periodic if there is a positive number T_1 from the domain of real numbers, i.e. $T_1 \in \mathbb{R}$ and $T_1 > 0$, such that for all real $t \in \mathbb{R}$ it holds that

$$s(t + T_1) = s(t) \tag{1.2}$$

This periodic signal is then denoted as $s_p(t)$ or $\tilde{s}(t)$. The lowest value of T_1 for which the condition (1.2) is satisfied is called the fundamental period. Periodic signals can further be classified into

– harmonic signals
– non-harmonic signals

The harmonic signal is defined using the cosine or the sine function. We use cosine

$$u(t) = U_m \cdot \cos\left(\frac{2\pi}{T_1} t + \varphi_1\right) \tag{1.3}$$

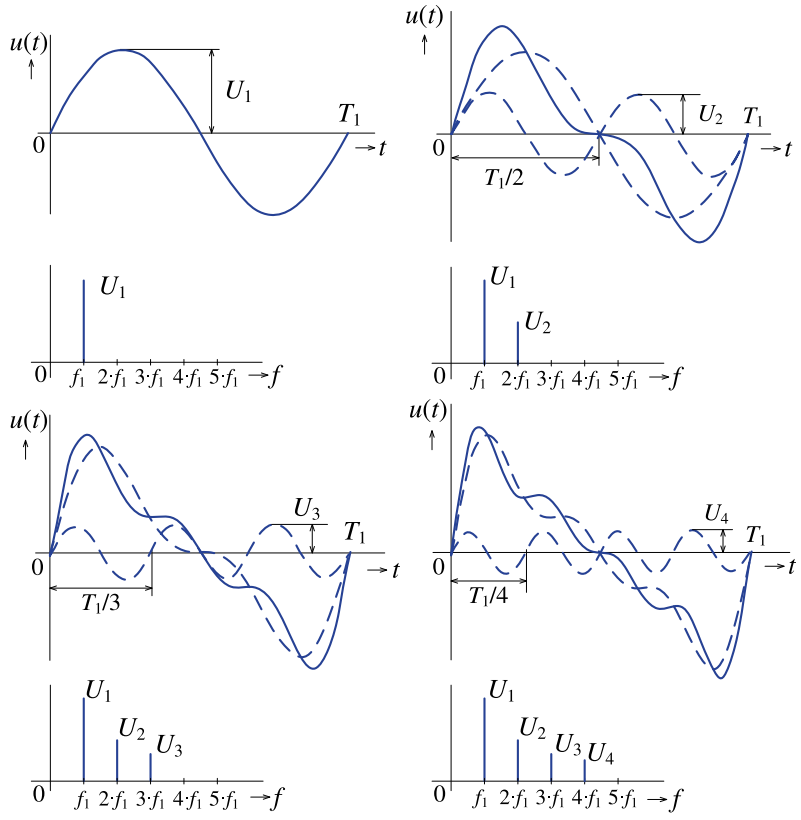

Figure 2.2: Successive addition of partial harmonic components in harmonic synthesis

Jean Baptiste Fourier (1768–1830) proposed for the first time the orthonormal system in his work on heat transfer by conduction (1823) and introduced a method which he called harmonic analysis. Those who contributed to the introduction of the Fourier series were Leonhard Paul Euler (1707–1783) and Daniel Bernoulli (1700–1782) with their work on the string. Alexis Claude Clairant (1713–1765) was the first to derive the Fourier series coefficients. In 1829, Johann Peter Gustav Lejeune Dirichlet (1805–1859) formulated sufficient conditions for expanding periodic functions into trigonometric series.

2.2 Definition of the Fourier series and its forms

There are several forms of the Fourier series and we will successively describe all of them. We will start with the mathematical definition [REK-94], [PAP-77].

Let $f(x)$ be a periodic function with a period of 2π, i.e. $f(x+2\pi)=f(x)$ for all x, and let $f(x)$ and $f'(x)$ be piece-wise continuous functions in the interval $<-\pi,\pi>$. Let us write

$$a_n=\frac{1}{\pi}\int_{-\pi}^{\pi} f(x)\cos nx\,\mathrm{d}x \quad \text{for } n=0,1,2,3,\ldots \tag{2.1}$$

$$b_n=\frac{1}{\pi}\int_{-\pi}^{\pi} f(x)\sin nx\,\mathrm{d}x \quad \text{for } n=1,2,3,\ldots \tag{2.2}$$

Then at every point x, at which $f(x)$ is continuous, it holds

$$\frac{a_0}{2}+\sum_{n=1}^{\infty}(a_n\cos nx+b_n\sin nx)=f(x) \tag{2.3}$$

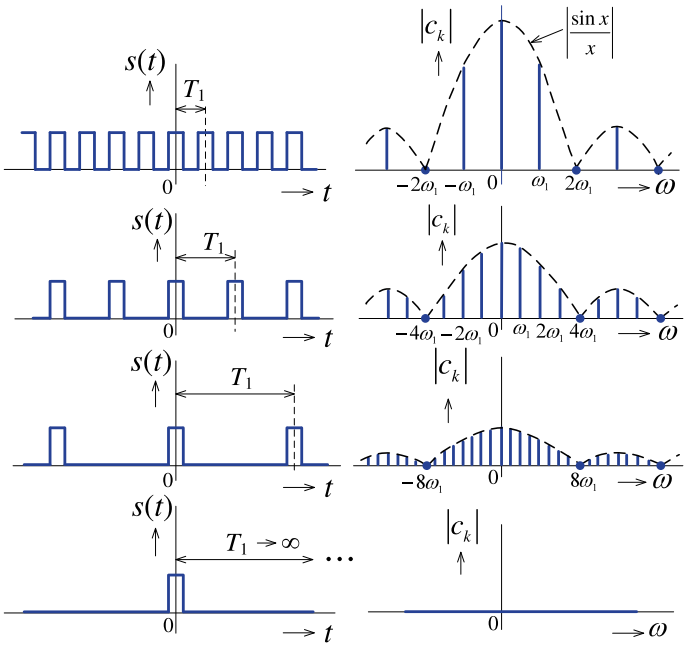

Figure 3.1: Periodic sequences of rectangular impulses and their spectrum of modules for different impulse-to-space ratios: 1: 1, 1: 3, 1: 7 *and* 1: ∞

The **inverse Fourier transform** (time function) is defined by the relation

$$s(t) = \frac{1}{2\pi} \int_{-\infty}^{\infty} S(\omega) \mathrm{e}^{\mathrm{j}\omega t} \mathrm{d}\omega \tag{3.4}$$

The definition of $S(\omega)$ is determined at the continuity points of $s(t)$. At the discontinuity points the integral converges to the arithmetic mean of the limit on the right and the limit on the left. Relations (3.3) and (3.4) can also be expressed as follows

$$S(\omega) = \mathcal{F}\{s(t)\}, \quad s(t) = \mathcal{F}^{-1}\{S(\omega)\}, \quad s(t) \Leftrightarrow S(\omega) \tag{3.5}$$

From (3.4) we can obtain the **Duality of the Fourier transform**. Let's first swap the variables t and ω and then by changing the sign of ω we get

$$s(\omega) = \frac{1}{2\pi} \int_{-\infty}^{\infty} S(t) \mathrm{e}^{\mathrm{j}t\omega} \mathrm{d}t$$

$$2\pi s(\omega) = \int_{-\infty}^{\infty} S(t) \mathrm{e}^{\mathrm{j}t\omega} \mathrm{d}t$$

$$2\pi s(-\omega) = \int_{-\infty}^{\infty} S(t) \mathrm{e}^{-\mathrm{j}t\omega} \mathrm{d}t = \mathcal{F}\{S(t)\}$$

Verbally: If $s(t)$ has Fourier transform $S(\omega)$, then $S(t)$ has Fourier transform $2\pi s(-\omega)$.

$$u_C(t) = U_0 \cos\ (\omega_0 t)\ , \qquad \omega_0 = \frac{1}{\sqrt{LC}} \tag{4.48}$$

In Fig. 4.17 we see the voltage and current waveforms of individual elements.

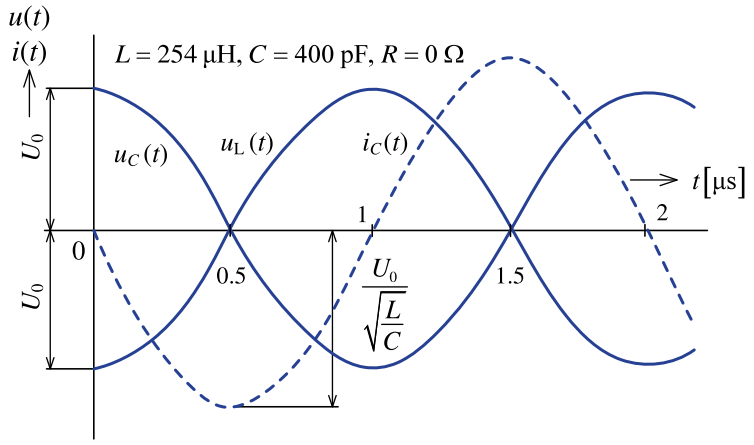

Figure 4.17: Voltage and current waveforms of the oscillating circuit from Fig. 4.13 for the non-attenuated waveform (characteristic equation roots are imaginary) [CAJ-56]

The inductor voltage and capacitor current are

$$u_L(t) = -U_0 \cos\ (\omega_0 t) \tag{4.49}$$

$$i_C(t) = C\frac{\mathrm{d}u_C(t)}{\mathrm{d}t} = C\frac{\mathrm{d}}{\mathrm{d}t}[U_0 \cos(\omega_0 t)] = \ \omega_0 C U_0 \sin(\omega_0 t) = U_0\sqrt{\frac{C}{L}}\sin(\omega_0 t) \tag{4.50}$$

For the specific chosen values $L = 254\ \mu\mathrm{H}$ and $C = 400\ \mathrm{pF}$ the frequency of natural oscillations (Thompson relation) is

$$f_0 = \frac{1}{2\pi\sqrt{LC}} = \frac{1}{2\pi\sqrt{2.54 \cdot 10^{-6} \cdot 4 \cdot 10^{-10}}} = 4.993134\ \mathrm{MHz}$$

4.7.3 First-order electric circuit with harmonic source

We will now show how to analyse an electric circuit where a source of harmonic voltage is connected. Again, we will choose a simple integrator circuit, the scheme of which is given in Fig. 4.18.

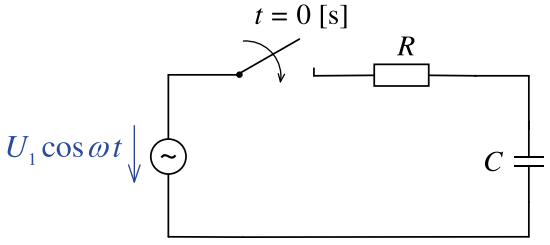

Figure 4.18: Connection of a first-order electric circuit with one accumulation element and harmonic excitation

The differential equation will be set up using equations of elements and circuits for the output quantity, which will be the capacitor voltage $u_C(t)$. The differential equation is defined by relation (4.5)

For $t \neq 0$ it holds

$$h(t) = \frac{1}{\omega_s} \int_{-\frac{\omega_s}{2}}^{\frac{\omega_s}{2}} e^{j\omega t}\, d\omega = \frac{1}{\omega_s} \left[\frac{e^{j\omega t}}{jt} \right]_{-\frac{\omega_s}{2}}^{\frac{\omega_s}{2}} = \frac{1}{\omega_s} \frac{e^{j\frac{\omega_s}{2}t} - e^{-j\frac{\omega_s}{2}t}}{jt} = \frac{2}{\omega_s t} \sin\frac{\omega_s}{2} t = \frac{\sin\frac{\omega_s}{2} t}{\frac{\omega_s}{2} t} \tag{5.17}$$

Now we are able to solve the equation (5.14)

$$s(t) = s_{id}(t) * h(t) = \left\{ \sum_{n=-\infty}^{\infty} s[nT]\delta(t - nT) \right\} * \frac{\sin\left(\frac{\omega_s}{2} t\right)}{\frac{\omega_s}{2} t}$$

$$= \int_{-\infty}^{\infty} \sum_{n=-\infty}^{\infty} s[nT]\delta(\tau - nT) \frac{\sin\left(\frac{\omega_s}{2}(t-\tau)\right)}{\frac{\omega_s}{2}(t-\tau)} d\tau$$

$$= \sum_{n=-\infty}^{\infty} s[nT] \int_{-\infty}^{\infty} \frac{\sin\left(\frac{\omega_s}{2}(t-\tau)\right)}{\frac{\omega_s}{2}(t-\tau)} \delta(\tau - nT) d\tau = \sum_{n=-\infty}^{\infty} s[nT] \frac{\sin\left(\frac{\omega_s}{2}(t-nT)\right)}{\frac{\omega_s}{2}(t-nT)}$$

where we have again exploited the sampling property of the Dirac impulse. The result is

$$s(t) = \sum_{n=-\infty}^{\infty} s[nT] \frac{\sin\left(\frac{\omega_s}{2}(t-nT)\right)}{\frac{\omega_s}{2}(t-nT)} \tag{5.18}$$

In Fig. 5.9 we see how spaces between discrete samples are filled and the original signal $s(t)$ is recovered.

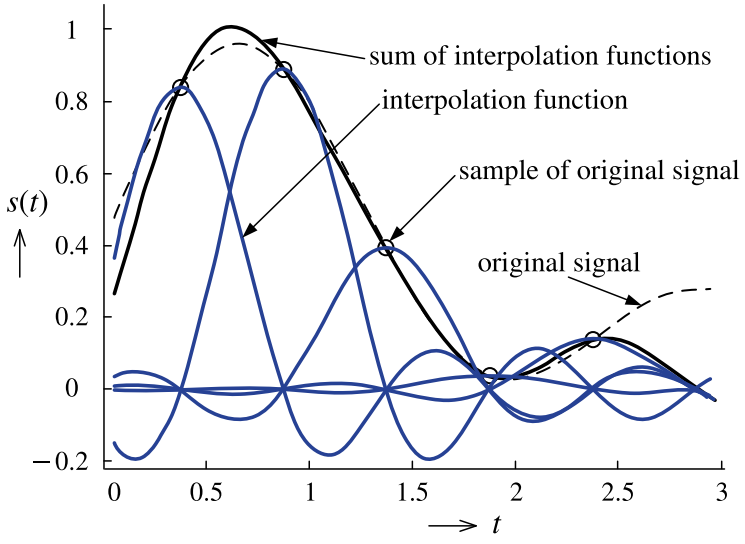

Figure 5.9: Recovering signal $s(t)$ from its samples $s[nT]$ using the ideal reconstruction lowpass filter in Fig. 5.8

It is obvious that the ideal lowpass filter (5.12) is a non-causal system. In practice, we must use a realizable low-pass filter (e.g. RC circuit in Fig. 4.5), and in that case the sampling theorem (5.11) can have the form

$$f_s > (\text{from } 2.35 \text{ to } 4) f_{max} \tag{5.19}$$

discrete signals, the next important factor, which influences the accuracy of the decomposition is the chosen sampling frequency. For envelope interpolation between discrete values of maxima and minima the cubic splines (of order 3) are usually employed. Their optimal adaptation during interpolation is carried out by means of genetic algorithms. As soon as the base components, which are real signals, are obtained, the Hilbert transform may be applied to calculate their analytic complex functions (sequences). From these functions instantaneous amplitude, instantaneous phase and instantaneous frequency are obtained. In Fig. 15.14a we can see the instantaneous amplitude of both base components and the unwrapped instantaneous phase of both components is illustrated in Fig. 15.14b. Unwrapping the phase is an operation which ensures the continuity of the phase, which can be found in non-unwrapped form only in the interval $\pm\pi$.

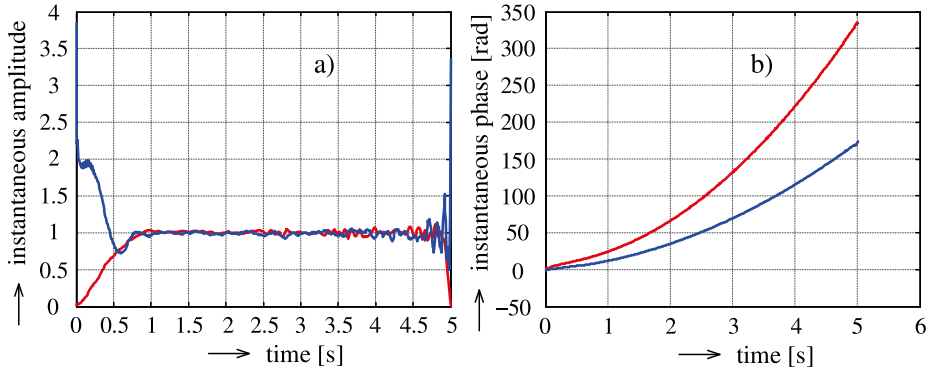

Figure 15.14: a) Instantaneous amplitude of both base components $c_1[n]$ (red) and $c_2[n]$ (blue), b) instantaneous unwrapped phase of base components $c_1[n]$ and $c_2[n]$

Instantaneous amplitude of both base components $c_1[n]$ and $c_2[n]$ should be equal to one. We can see that errors occur at the beginning and at the end of the frames. These errors can be partially minimized by optimizing the interpolation of maxima and minima by means of the cubic splines. In Fig. 15.15 we can see the instantaneous frequency of both base components. Also here, except of the beginning and final part of the interval, the change of frequency in time nearly corresponds to the sweep of the cosine waves according to relation (15.36). In such a way we obtain more precise results than it was in the case of the spectrogram shown in Fig. 15.12b.

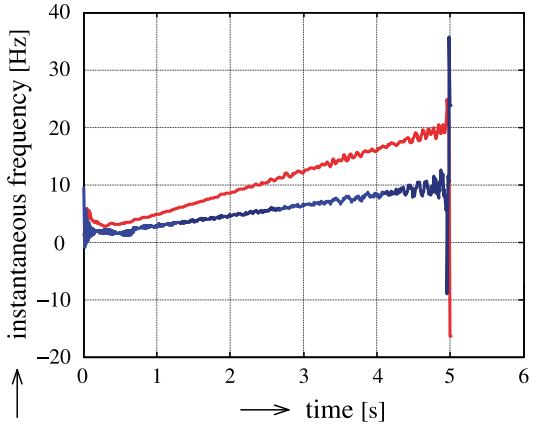

Figure 15.15: Time responses of instantaneous frequency of the base components $c_1[n]$ (red) and $c_2[n]$ (blue)

- the mother wavelet can be of non-zero value only in a finite interval (or non-zero values must be negligible outside this finite interval)

$$\int_{-\infty}^{\infty} t^k \psi(t) \mathrm{d}t = 0$$

- derivations up to the m-th order (order of the wavelet) of the mother wavelet must be continuous, by increasing the scale the values of coefficients must get smaller and thus for decomposition a lower number of the coefficients is required
- there must exist an inverse transform, to define the inverse transform, the following condition must be satisfied

$$\int_{-\infty}^{\infty} \frac{|\Psi(\omega)|^2}{\omega} \mathrm{d}\omega < \infty$$

$\Psi(\omega) = \mathcal{F}\{\psi(t)\}$, where the symbol $\mathcal{F}\{\cdot\}$ denotes the Fourier transform.

Let us assume that the mother wavelet $\psi(t) = \psi_{0,0}(t)$ begins at $t = 0$ and ends at $t = \tau$. The shifted wavelet $\psi_{0,q}(t)$ begins at $t = q$ and ends at $t = q + \tau$

$$\psi_{0,q}(t) = \psi(t - q) \tag{16.1}$$

The expanded (compressed) wavelet $\psi_{p,0}(t)$ begins at $t = 0$ and ends at $t = \tau p$

$$\psi_{p,0}(t) = \frac{1}{\sqrt{|p|}} \psi\left(\frac{t}{p}\right) \tag{16.2}$$

The factor $1/\sqrt{|p|}$ ensures energy normalization (the energy of expanded or compressed wavelets remains the same). If $p < 1$ compression in time occurs, e.g. for $p = 0.5$ we have $\psi(t/0.5) = \psi(2t)$. If $p > 1$, we obtain the expanded mother wavelet. The example is for $p = 2$ as $\psi(t/2) = \psi(0.5t)$. The wavelet $\psi_{p,q}(t)$ which is compressed or expanded p-times and shifted in time by q, is of the following form:

$$\psi_{p,q}(t) = \frac{1}{\sqrt{|p|}} \psi\left(\frac{t - q}{p}\right) \tag{16.3}$$

The important characteristic which the bases of wavelets functions should satisfy is **orthogonality**. The base of wavelet functions will be orthogonal if the scalar product of two non-identical wavelets is zero, i.e.

$$< \psi_{p,q}(t), \psi_{r,s}(t) > = \int_{-\infty}^{\infty} \psi_{p,q}(t)\, \psi_{r,s}^*(t)\, \mathrm{d}t = 0 \tag{16.4}$$

when $p \neq r$ or $q \neq s, r \in \mathbb{R}, s \in \mathbb{R}, p \in \mathbb{R}, q \in \mathbb{R}$. A complex continuous-time function $s(t)$ can be expressed as a linear combination of the wavelets

$$s(t) = \sum_p \sum_q b_{p,q}\, \psi_{p,q}(t) \tag{16.5}$$

The coefficients $b_{p,q}$ are the weights by which the individual wavelets $\psi_{p,q}(t)$ contribute to the formation of the signal $s(t)$. Now we multiple both sides of the equation (16.5) by the complex conjugated wavelet $\psi_{r,s}^*(t)$ and integrate

$$\int_{-\infty}^{\infty} s(t)\, \psi_{r,s}^*(t) \mathrm{d}t = \int_{-\infty}^{\infty} \left\{ \sum_p \sum_q b_{p,q}\, \psi_{p,q}(t) \right\} \psi_{r,s}^*(t) \mathrm{d}t = b_{r,s} \int_{-\infty}^{\infty} |\psi_{r,s}(t)|^2 \, \mathrm{d}t \tag{16.6}$$

Comparing the values ψ_{dB4} and $g_1[n]$, we see that

$$g_1[n] = \frac{1}{\sqrt{2}}\psi_{\mathrm{dB4}} \tag{16.30}$$

Similarly, comparing the values φ_{dB4} and $g_0[n]$, we see that

$$g_0[n] = \frac{1}{\sqrt{2}}\varphi_{\mathrm{dB4}} \tag{16.31}$$

The equation (14.22) in Chapter 14 gives the first condition of the perfect reconstruction of the causal two-channel QMF bank

$$G_0(z)H_0(z) + G_1(z)H_1(z) = 2$$

The second condition is then

$$G_0(z)H_0(-z) + G_1(z)H_1(-z) = 0$$

The proper form of the conditions of the perfect reconstruction of the causal QMF bank which corresponds to the orthonormal system of the wavelet and scaling functions should be

$$\frac{1}{\sqrt{2}}G_0(z)\frac{1}{\sqrt{2}}H_0(z) \; + \; \frac{1}{\sqrt{2}}G_1(z)\frac{1}{\sqrt{2}}H_1(z) = 1 \tag{16.32}$$

$$\frac{1}{\sqrt{2}}G_0(z)\frac{1}{\sqrt{2}}H_0(-z) + \frac{1}{\sqrt{2}}G_1(z)\frac{1}{\sqrt{2}}H_1(-z) = 0 \tag{16.33}$$

In Fig. 16.12 module frequency responses of Daubechies wavelets for different orders are depicted. The higher the order of the wavelet, the steeper the response from the band-stop range to the band-pass range.

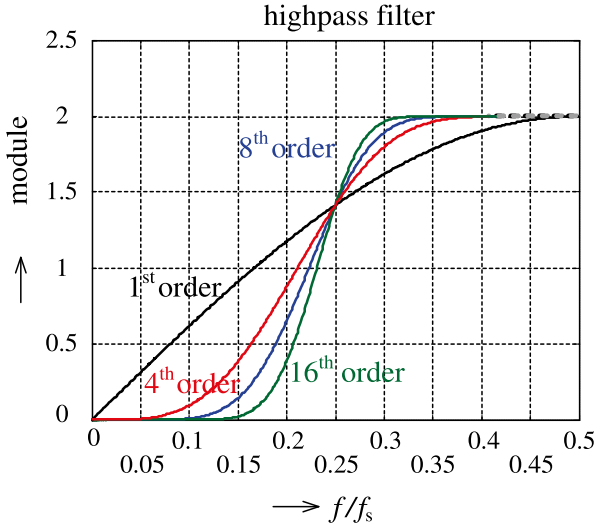

Figure 16.12: Module frequency responses corresponding to Daubechies wavelets of the 1st, 4th , 8th and 16th order

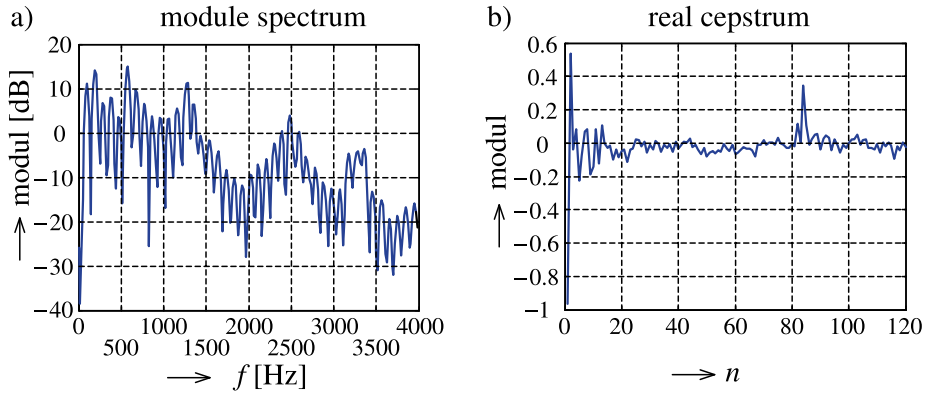

Figure 18.10: a) module spectrum of the vowel [a] represented as its envelope, b) real cepstrum of the vowel [a]

There is a function **`recps`** in Matlab to calculate the real cepstrum. In the real cepstrum shown in Fig. 18.10b we can see the impulse for the approximate value of $n = 83$. This corresponds to the frequency of the pitch of speech for the vowel [a] $\frac{f_s}{n} = \frac{8000}{83} = 96.38$ Hz. Using the homomorphic deconvolution it is possible to determine from the real cepstrum both the frequency response of the vocal tract (for $f_s = 8$ kHz, 25 cepstral coefficients are sufficient) and the parameters of the exciting signal.

18.3.3 Approximation of exponential function using continued fraction expansion

Once we want to perform the cepstral transform in any hardware equipment, we can come across the problem that we do not have sufficient memory space, or the computing power is too low. Then we have to try to substitute the exponential function in the inverse cepstral transform by another suitable model. As a possible solution, expansion of the exponential function using continued fraction expansion can be applied. Similarly as other transcendent functions, the exponential function can be expanded into continued fractions in the following way [CHOV-56]

$$e^x = \cfrac{1}{1-\cfrac{x}{1+\cfrac{x}{2-\cfrac{x}{3+\cdots+\cfrac{x}{2-\cfrac{x}{2s-1+\cdots}}}}}} = \frac{1}{1} - \frac{x}{1} + \frac{x}{2} - \frac{x}{3} + \cdots + \frac{x}{2} - \frac{x}{2s-1}\cdots \tag{18.46}$$

Infinite expansion into continued fractions is then formally denoted by the symbols + or −, which are located below the fraction line. Other functions can be represented as

$$\ln(x) = \frac{2(x-1)}{x+1} - \frac{(x-1)^2}{3(x+1)} - \cdots - \frac{s^2(x-1)^2}{(2s+1)(x+1)} - \cdots$$

$$\arctan(x) = \frac{x}{1} + \frac{x^2}{3} + \frac{4x^2}{5} + \cdots + \frac{s^2x^2}{(2s+1)} + \cdots$$

$$\sqrt{x} = 1 + \frac{x-1}{2} + \frac{x-1}{2} + \frac{x-1}{2} + \cdots$$

The approximation accuracy of transcendent functions depends on the number of terms in the expansion into continued fractions, i.e. on the order s. For example, while approximating the exponential function (18.46), the sequences of the rational fraction functions which have a higher number of terms, i.e. a higher value of s, increase the accuracy of approximation as follows

In the *i2920* assembler, the program for the implementation of equations (21.14) with the coefficients (21.8) will be of the following form

```
; calculation of the output value y[n]
LDA X, DAR ;        the input value from the A/D converter is saved into the X register
LDA Y, V ;          y[n] = v[n − 1]
ADD Y, X, R05 ;     y[n] = 2^−5 x[n] + v[n − 1]
SUB Y, X, R10 ;     y[n] = (2^−5 − 2^−10) x[n] + v[n − 1]
ADD Y, X, R12 ;     y[n] = (2^−5 − 2^−10 + 2^−12) x[n] + v[n − 1]
LDA DAR, Y ;        the output value goes into the D/A converter via the DAR register
; - - - - - - - - - - - - - - -
; preparation of the state-space variable for calculation in the next sampling interval
LDA V, X, R05 ;     v[n] = 2^−5 x[n]
SUB V, X, R10 ;     v[n] = (2^−5 − 2^−10) x[n]
ADD V, X, R12 ;     v[n] = (2^−5 − 2^−10 + 2^−12) x[n] = c1 x[n]
SUB V, Y ;          v[n] = c1 x[n] + (−2^0) y[n]
ADD V, Y, R05 ;     v[n] = c1 x[n] + (−2^0 + 2^−5) y[n]
SUB V, Y, R09 ;     v[n] = c1 x[n] + (−2^0 + 2^−5 − 2^−9) y[n]
ADD V, Y, R12 ;     v[n] = c1 x[n] + (−2^0 + 2^−5 − 2^−9 + 2^−12) y[n]
ADD V, Y, R13 ;     v[n] = c1 x[n] + (−2^0 + 2^−5 − 2^−9 + 2^−12 + 2^−13) y[n] = c1 x[n] + d1 y[n]
```

We see that the complexity of the coefficients determines the program length. This procedure can be employed in microprocessors which do not have a hardware multiplier in their structure.

21.3 Implementing first-order LTI discrete systems in microprocessors with hardware multiplier

Other types of microprocessors (not only digital signal processors) often have in their architecture a built-in hardware multiplier and then it is not necessary to conduct multiplication via a program. As an example we have chosen the DSP56300 digital signal processor (Motorola). The **Harvard architecture** is a type of digital signal processors made by Motorola, Freescale and other companies. The structure of the arithmetic-logic unit (ALU) of the fixed-point DSP56300 digital signal processor can be seen in Fig. 21.6.

The advantage of the existence of a hardware multiplier is that the program length in the assembler does not depend on the coefficients complexity. As can be seen in Fig. 21.7, the coefficients, the input and output samples, and the state-space variables are stored in the X: and Y: memories.

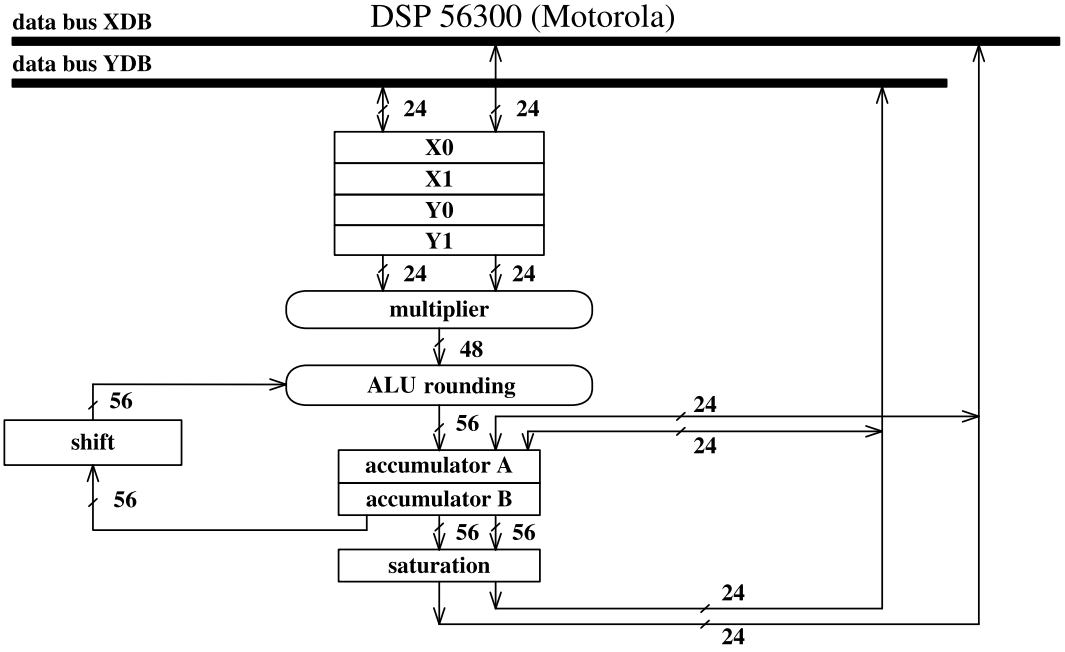

Figure 21.6: Data arithmetic-logic unit of the fixed-point digital signal processor with Harvard architecture